JOURNAL OF MATERIALS SCIENCE **36** (2001) 5369–5377

The effects of composition and processing variables on the properties of thermoplastic polyaniline blends and composites

H. MORGAN*, P. J. S. FOOT
Materials Research Group, Faculty of Science, Kingston University, Penrhyn Road, Kingston upon Thames, Surrey KT1 2EE, UK
E-mail: h.morgan@kingston.ac.uk

N. W. BROOKS
School of Polymer Technology, Faculty of Science, Computing and Engineering, University of North London, 166-220 Holloway Road, London, N7 8DB, UK

Pure polyaniline (PANI) has a high electrical conductivity and can be made soluble and thermoplastic, but it still lacks adequate mechanical properties for large-scale commercial use and therefore, it has been blended with other polymers such as poly(methyl methacrylate) (PMMA). In the work described in this paper, the scaled up synthesis of conductive polyaniline by an oxidative chemical method under controlled pH and temperature has been optimised. Re-doping of deprotonated insulating base with excess of the mono-functional organic acids such as p-toluenesulfonic (TSA) or dodecylbenzenesulfonic (DBSA) in aqueous media was successful. A wide range of techniques including TGA, GPC, EA, FTIR, XRD and SEM were employed for the characterisation of PANI powders and blends. Compositions of PANI-HCl, TSA or DBSA and thermoplastic matrix PMMA with or without a plasticiser were melt-processed by compression moulding for 3 min at 210°C to produce plaques. The effectiveness of four different phenolic plasticisers was compared and hydroquinone was found to produce the blends with the highest conductivities. A few preliminary injection-moulded plaques were made and their conductivities were compared with those of the compression-moulded samples.

1. Introduction

A new class of conductive materials called "organic synthetic metals" such as polyaniline has been the subject of intensive research and development for a number of years. Several reviews on existing, and newly developed polymers, have been published [1, 2].

Conductive polyanilines are easy to synthesise, and relatively thermally stable. Polyaniline can be used in electromagnetic shielding, for antistatic charge dissipation, printed circuit boards for electronics applications, in conductive fabrics in textile industry, and for the corrosion protection of metals such as iron [3].

Various syntheses of polyaniline have been described in the literature including oxidative chemical, electrochemical and emulsion polymerisation [4, 5]. The process of making polyaniline conductive is called doping which involves either protonation or partial oxidation or reduction via counter-anions entering or leaving the polymer. Doped polyanilines have low solubilities in conventional organic solvents, which make their processing very difficult. This can be resolved by doping deprotonated PANI (emeraldine base EB) with functional organic acids such as TSA, DBSA, or CSA, which can render the polymer thermoplastic. PANI is quite thermally stable, but may lose conductivity at high temperatures due to loss of dopant. Conductivity values in the literature are in the range 1–10 S cm^{-1} for pure polyaniline and around 10^{-3}–10^{-7} S cm^{-1} for PANI-blends [6–8]. Polyaniline composites can be prepared by direct polymerisation within a matrix polymer, but since both the monomer and the polymerisation agent must be able to diffuse into the matrix, this may be difficult. Moreover, the blend will not usually be processable afterwards without losing its conductivity.

Poly(methyl methacrylate) was chosen here as a thermoplastic partner for PANI-blends because it is freely available, easily processed and possesses similar polarity to PANI with a convenient T_g. PMMA is well suited for the preparation of transparent conductors by blending with PANI due to its low absorptivity in the visible region. Moreover, it was expected to allow the PANI to form an interpenetrating network containing conducting pathways. Two techniques have been used to ease the process of mixing PANI with

*Author to whom all correspondence should be addressed.

common structural polymers have been successfully used [9, 10]: (a) dispersing; in which intensive mixing and a "dispersing agent" are used to disperse the PANI within the host polymer, (b) plasticising; in which a "plasticiser" is added to PANI to soften it and hence make it more processable. When PANI is doped with an excess of DBSA, not only does the DBSA dope the PANI, it also plasticises it, decreasing the transition temperature and producing protonated, melt processable complexes. The protonation is expected to take place probably on the iminic nitrogen sites (the oxidised part of polyaniline chain).

Processing techniques for polyanilines can be divided into: (a) those involving melt processing and dry mixing such as extrusion, injection or compression moulding, and (b) solution processing methods such as casting or spraying. To improve the processibility of polyaniline, use may either be made of counter-ion induced solubility, or of dispersing the insulating emeraldine base in a suitable solvent and mixing the dispersion with a solution of a matrix polymer such as PMMA, followed by post-doping after blending in order to obtain appreciable conductivities.

The aims of the present study were to understand the correlation between the composition and flow related properties of PANI-blends and their electrical conductivities. Although the best conductivities obtained were for compression-moulded plaques, the possibility of processing by injection/transfer moulding is currently being investigated in our laboratory.

2. Experimental

2.1. Materials

Aniline 99% and ammonium persulphate 98% (both Sigma-Aldrich) and hydrochloric acid (BDH, 35–38%) were used to synthesise emeraldine salt (PANI-HCl) by oxidative chemical polymerisation. Some of the emeraldine base (EB), non-conducting form of polyaniline, was prepared by de-protonating PANI-HCl in ammonia solution (BDH, 35% NH_3). Re-doping EB was carried out in aqueous media of p-toluenesulfonic acid (98%, BDH) or dodecylbenzenesulfonic acid (Alfa, Johnson Matthey 97%) to prepare two types of conductive doped polyaniline PANI-TSA and PANI-DBSA. The matrix polymer, PMMA (ICI powder-MG102D, clear grade) was used for preparing PANI blends with numerous plasticiser; hydroquinone, resorcinol, tert-butyl hydroquinone, 4-hexyl resorcinol (Sigma-Aldrich, 99, 98, 97 and 99% respectively) and bisphenol-A (BDH, industrial grade).

2.2. Synthesis of polyaniline

Conductive emeraldine salt PANI-HCl (approximately 400 g) was synthesised by an oxidative chemical polymerisation at a molar ratio of 0.1 aniline (ANI) to 0.125 ammonium persulphate (APS) [11]. The APS (1257 g, 0.125 mole) was dissolved in 1 M HCl (3520 ml), which had been precooled to 1°C. The ANI (400 ml, 0.1 mole) was dissolved in 1 M HCl (4400 ml) and also precooled to 1°C. The ANI solution was placed in an ice bath with an overhead-stirrer. The APS solution was added to the ANI solution over a period of 20 min with constant stirring to ensure thorough mixing. A few drops of $FeCl_3$ were added to the polymerisation mixture as a catalyst. The temperature of the polymerisation mixture was maintained below 0°C, while the pH was adjusted to 0–0.5 by the addition of concentrated HCl. The mixture was left to stand for 5 days to complete the polymerisation and to settle before decanting and finally washing with distilled water until the filtrate was colourless. EB was prepared by de-protonating the wet emeraldine salt (PANI-HCl) in 35% aqueous ammonia solution (4500–6000 ml) with 24–170 h stirring followed by the protonation in aqueous solutions of TSA or DBSA at a molar ratio of EB:TSA or EB:DBSA of 1:0.5. Filtration was carried out using filter paper (Whatman grade 3 with particle retention of 6 μm), which took a minimum of 72 h. All products were washed with large quantities of distilled water until filtrates were colourless and no odour of ammonia could be detected, and the precipitates remained under suction until cracks in the filter cakes started to appear. Drying was carried out in a vacuum oven at a temperature of 40°C for PANI-HCl, and 75°C for PANI-TSA and PANI-DBSA.

2.3. Blending and processing

A compression-moulder (Tangeys Ltd) with temperature controller (Guardsman) and an injection-moulder (GKN machinery Ltd) were employed. At the beginning of the project, three processing methods were investigated: (a) Hand mixing of PANI powders with PMMA followed by compression moulding, (b) Hand mixing of PANI powders with PMMA followed by twin-screw extrusion and then compression moulding and (c) Hand mixing of PANI powders with PMMA followed by injection moulding. Of these only method (a) produced measurable conductivities, so a series of different compositions of PANI-HCl, PANI-TSA and PANI-DBSA powders with PMMA were mixed in a coffee blender, with or without the addition of a plasticiser. These blends were melt-processed between 180–210°C (depending on the dopant) by compression moulding for about 3 min producing plaques. A few preliminary injection-moulded samples were also made.

2.4. Characterisation

2.4.1. Spectroscopy

FT-IR spectra in the range 4000–400 cm^{-1} were recorded on KBr pellet samples, using a Perkin Elmer, Paragon 1000 Spectrometer. For the absorption spectra in the UV-visible range (wavelength 900–361 nm), a Cary 100 spectrophotometer was employed. For ^{13}C and ^{1}H NMR analyses of solutions, a Bruker AC 300F was utilised.

2.4.2. Thermal analysis

Dehydration, loss of dopant and backbone degradation of all PANI powders were investigated by thermogravimetric analysis (Perkin Elmer TGA 7). TGAs were carried out in air or under nitrogen atmosphere from 25 to 320°C at a heating rate of 25°C/min. Some differential

scanning calorimetric experiments using a Mettler DSC 25 were also performed under nitrogen atmosphere at 10°C/min to study endothermic and exothermic reactions, phase changes and glass transitions.

2.4.3. Conductivity measurements

Electrical conductivity measurements were performed using the van der Pauw four-probe technique [12] (with Ag contacts) for pure PANI-salt powders as pellets (14×1.5 mm) and for PANI blends as plaques ($90 \times 90 \times 1.5$ mm). Samples were connected to a Keithley 617 programmable electrometer and Keithley 224 programmable current source under computer control. For less conductive plaques (conductivity levels $<10^{-7}$ S cm^{-1}), 2-probe measurements were performed after coating opposite faces of the plaque with quick-drying silver paint. The van der Pauw equation (1) below was used to calculate conductivities;

$$\sigma = \frac{2 \ln 2}{(R_1 + R_2)\pi d f} \quad (1)$$

Where σ is conductivity (S cm^{-1}), R_1 & R_2 are resistances of the sample in two adjacent configurations, d is thickness of the sample (cm), and f is geometric correction factor (approximately 1.00 for circular pellets or square shaped plaques). Surface conductance was not found to be significant (i.e. the values measured were true bulk conductivities).

2.4.4. Molecular weight measurements

Gel-permeation chromatography (GPC) molecular-weight measurements of PANI samples were calibrated with mono-dispersed polystyrene standards using a Waters GPEL GPC column with a 996 Photodiode Array Detector, Waters 600 controller and pump. The PANI solution was prepared as follows; ca. 1–2 wt% of polyaniline stirred for 4 days in 10 ml of tetrahydrofuran (THF) with 1 μl of toluene (as an internal marker), centrifuged and finally filtered through cotton wool or a sintered disc with 0.5 μm porosity. The GPC column and detector were maintained at 35°C and 30°C, respectively. The calibration with polystyrene standards (Sigma-Aldrich) was carried out under identical conditions to the PANI solution analysis.

2.4.5. Morphological characterisation

X-ray powder diffraction analysis was carried out using an automated Philips diffractometer PW1730/10 model with Ni filtered Cu K_α radiation ($\lambda = 1.54$ Å). The diffractometer was operated at 40 kV and 30 mA and diffraction patterns of PANI powders were recorded over the range of 2θ between 3–50° (counting time 5 s and step size 0.05°). Samples were mounted on a standard Philips aluminium holder.

Particle size distribution of PANI powders was measured using a Coulter counter Industrial model D. Scanning electron microscopy (SEM) using a JEOL JSM 6310 with an accelerating voltage of 15 kV was carried out on PANI plaques to study their morphologies. Specimens were either gold sputtered or carbon coated prior to examination.

3. Results and discussion

3.1. PANI powders

3.1.1. Elemental analysis

Elemental analyses tabulated below were carried out by Medac Ltd. Theoretical % compositions were calculated and compared with the experimental values. (The experimental O percentages in PANI-TSA and PANI-DBSA were calculated by difference, as is customary).

EB

Element	C	H	N
% Theory	79.55	4.97	15.46
% Found 1	73.21	4.47	14.20
% Found 2	73.08	4.43	14.19

From average results, the empirical formula is calculated to be $C_{12}H_{8.9}N_{2.00}$, which agrees very well with the theoretical $C_{12}H_9N_2$ for emeraldine base [4].

PANI-HCl

Element	C	H	N	Cl
% Theory	66.20	4.59	12.87	16.32
% Found 1	57.73	4.23	10.93	14.40
% Found 2	57.84	4.17	10.96	14.51

From the average results the empirical formula is calculated to be $C_{12}H_{10.39}N_{1.94}Cl_{1.01}$, which is in excellent agreement with the theoretical $C_{12}H_{10}N_2Cl$. The atomic ratio of Cl to N is 0.52, (i.e. 52% protonation). The degree of protonation in PANI-HCl has been reported to be between 42–50% [4].

PANI-TSA

Element	C	H	N	S	O	Total
% Theory	64.58	4.81	7.93	9.06	13.60	100
% Found 1	59.47	5.23	7.44	8.47	19.39	100
% Found 2	59.34	5.21	7.56	8.74	19.51	100

The empirical formula calculated from the average results is $C_{19}H_{19.87}N_{2.05}S_{1.03}O_{3.26}$, which is slightly higher in H and O % than the theoretical $C_{19}H_{17}N_2SO_3$. This can be attributed to the presence of water (since TSA is slightly hygroscopic) and to the possibility that PANI-TSA was slightly less oxidised than expected. The atomic ratio of S to N is 0.50, (i.e. 50% protonation).

PANI-DBSA

Element	C	H	N	S	O	Total
% Theory	68.32	6.56	6.51	7.45	11.16	100
% Found 1	67.89	6.93	6.24	5.71	13.23	100
% Found 2	67.61	6.93	6.24	5.75	13.47	100

The theoretical formula is $C_{30}H_{39}N_2SO_3$ and the empirical formula from the average found results is $C_{30}H_{36.5}N_{2.37}S_{0.95}O_{4.42}$, slightly lower in H and lower in S, which is thought to be due to water being present and to the polymer being slightly under oxidised. The atomic ratio of S to N is 0.40 (i.e. 40% protonation).

TABLE I Assignments of the main peaks in the FTIR spectra (cm^{-1}) of PANI powders in KBr discs

Peak assignment	EB	PANI-HCl	PANI-TSA	PANI-DBSA
N–H Str.	3385	–	3427, 3228	3448
Aliphatic Str.	2361	2343	2373	2923, 2852, 2360
N=Q=N Str.	1588	1588	1560	1559
N–B–N ring Str.	1497	1473	1476	1474
Q=N–B Str.	1378	1302	1299	1300
C_{ar}–N Str.	1306	1244	1242	1242
C–H Bend	1165	1132	1120, 1132	1121
C–H Bend	956, 831	880, 805	880, 802	881, 800
C–C Bend	669, 648	704, 670	707, 679	706, 683, 669
C–C Bend	503, 418	594, 502	560, 563, 508	579, 504, 418
S=O Str.	–	–	1030, 1006	1031, 1006

Note: Str. = stretching, Bend = bending, B = benzene and Q = quinoid ring.

3.1.2. Spectroscopic measurements

3.1.2.1. FTIR. A summary of all the FT-IR spectra for EB, PANI-HCl, PANI-TSA and PANI-DBSA is given in Table I. All these results are in full agreement with the literature values [5, 13, 14]. Typical IR peak positions for benzoid (N–B–N) and quinoid structural units (N=Q=N) are around 1500 and 1600 cm^{-1} respectively.

3.1.2.2. UV-visible. The electronic conduction in polyaniline arises from the protonation of imine nitrogens, leading to the formation of large polarons. The UV-visible spectrum of the deprotonated, fully reduced EB after stirring in THF for 3 days showed two absorption bands peaking at 588 and 323 nm. These can be attributed to the (π-π^*) excitation of benzenoid and quinoid segments (charge-transfer exciton-like transition from the HOMO to the LUMO on the benzenoid and quinoid rings in the polyaniline chains respectively). A weak, broad band at 900 nm and a strong, sharp band at 335 nm have previously been reported for the fully-reduced form of polyaniline [15]. For PANI-HCl left stirring in THF overnight and filtered through cotton wool, the solution was very pale green. Its UV-visible spectrum showed only one absorption band at 368 nm. The UV-visible spectrum of PANI-TSA showed one absorption band at 375 nm. Two peaks, 790 and 368 nm have been assigned for the bright green-coloured solution of PANI-DBSA. The polaron peak resulting from the doping of the polymer can be usually found around 780–800 nm, a characteristic feature of a localised polaron at ~800 nm.

3.1.2.3. NMR. Solutions of EB and PANI-DBSA in dimethylsulphoxide (DMSO) were scanned. For proton nmr, peaks corresponding to aromatic H at 6.99 ppm and non-aromatic H at 3.34 and 1.2 ppm could be assigned. Similarly for PANI-DBSA, (^{1}H) disubstituted aromatic H of SO_3H-benzene-CH_2, CH_3 and CH peaks at 7–7.6 and 0.6–1.6 ppm respectively, were observed.

Polyaniline powders gave complicated solution-state carbon-13 NMR spectra mainly due to their limited solubilities in common organic solvents. It appears that at least 5000–30000 scans may be required for a satisfactory NMR analysis [16].

3.1.3. Thermal analysis

3.1.3.1. TGA. From Table II, it can be seen that under N_2, the weight loss for all heated samples was slow compared with that in air. From room temperature to 120°C, the weight loss was due to evaporation of water for all polymers EB, PANI-HCl, PANI-TSA and PANI-DBSA. Emeraldine base was stable at least up to 200°C, the maximum temperature set here for this material, but its stability has been reported to be up to 400°C [17]. PANI-HCl was relatively stable until deprotonation started at about 100°C and continued up to 500°C, which was then followed by backbone degradation. PANI-TSA was stable until 260–300°C, when loss of dopant occurred, followed by degradation

TABLE II Thermogravimetric data for PANI powders

Polymer	Temp (°C) & 1st wt loss%	Temp (°C) & 2nd wt loss%	Total wt loss% for 1st + 2nd stages	Temp (°C) & 3rd wt loss%
EB				
In N_2	25–120, 7.8	120–150, 0.1	7.9%	150 + stable
PANI-HCl				
In air	25–120, 11	120–300, 5	16%	300 + cont. loss
In N_2	25–120, 7.5	120–300, 8.5	16%	300 + cont. loss
PANI-TSA				
In air	25–120, 5	120–260, 2	7%	260 + sharp loss
In N_2	25–120, 4.5	120–300, 0.5	5%	300 + sharp loss
PANI-DBSA				
In air	25–120, 3	120–260, 1	4%	260 + sharp loss
In N_2	25–120, 1.5	120–320, 0.5	2%	320 + sharp loss

of the main chain. PANI-DBSA was more stable than PANI-HCl, but deprotonation followed by degradation of the aliphatic side-chain of DBSA started between 260–320°C. Similar results were reported by Gazotti and Kim [7, 14].

3.1.3.2. DSC. Thermal stability of the polyanilines appears to be influenced by the type of dopant; small ones such as HCl can be easily removed by heating, whereas large molecules e.g. TSA or DBSA, are more strongly bound. DSC showed a large endothermic peak attributed to the loss of water between 30–150°C for the emeraldine base. For PANI-HCl, three peaks have been identified, namely a small-medium endotherm between 30–100°C due to loss of water followed by a second endotherm between 100–260°C due to deprotonation and the third (exothermic) above 280°C associated with the PANI's backbone degradation. PANI-TSA lost free water between 30–65°C, deprotonated between 80–330°C and started to degrade between 330–390°C. For PANI-DBSA, loss of water occurred between 30–65°C and deprotonation above 200°C. It has not been possible to identify the T_g of the PMMA or PANI samples, but literature T_g values quoted are 99.8°C for pure PMMA and 108.7°C for PANI-PMMA (dry blend) [18].

3.1.4. Molecular weight measurements

High molecular weight polyaniline was obtained as a result of controlled pH and temperature of polymerisation. The molecular weight data for EB in this work is comparable with a literature value, $\bar{M}_n$ of ca. 7300, similarly measured by GPC with polystyrene calibration [19]. Due to their limited solubilities, the molecular weight distribution was not fully sampled for PANI-HCl and PANI-TSA. However, EB and PANI-DBSA were more soluble and therefore gave reasonable values, (see Table III). After dissolution for 1 h in THF, PANI-DBSA gave an $\bar{M}_n$ of 21000, which is roughly what would be expected from the $\bar{M}_n$ observed for EB. However, an aged solution (4 days) showed a much larger $\bar{M}_n$, which can only be due to agglomeration into particles such as those seen by SEM.

3.1.5. Morphological characterisation

3.1.5.1. XRD. It appears from the X-ray diffraction patterns presented in Fig. 1, that the degree of crystallinity of PANI powders is relatively low. The aluminium holder used to mount the PANI samples gave three sharp peaks at $2\theta = 37°$, 44° and 77°, which should be disregarded. Three common reflections for all PANI powders were recorded; a strong peak at 65°,

TABLE III Molecular weight measurements (GPC) for all PANI powders

Sample	$\bar{M}_n$	$\bar{M}_w$
EB	6000	11000
PANI-HCl	3000	4000
PANI-TSA	3500	5000
PANI-DBSA, Fresh solution	21000	22000
Aged solution	580000	1030000

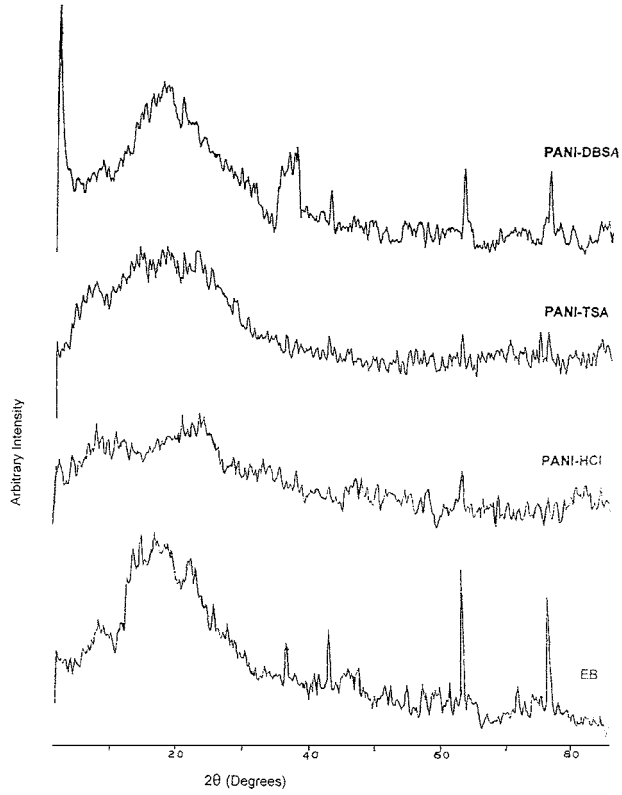

Figure 1 XRD patterns of EB, PANI-HCl, PANI-TSA and PANI-DBSA powders.

a broad reflection at $2\theta = 15$–27° corresponding to the amorphous region and finally a small one at about 10°. PANI-DBSA was found to have a partially crystalline structure, probably because of the bulky dopant present in the lattice causing some self-organisation. In addition to the common reflections, there is an additional strong peak at $2\theta = 3.5°$ (d-spacing about 25 Å), which is characteristic of an interlayer repeat distance of alkyl tails of counter-ions that function as spacers between parallel planes of stacked PANI backbone [13, 17]. It is also possible that careful annealing can further increase crystallinity and conductivity of this material.

3.1.5.2. Particle size analysis. The average particle size of EB was 12 μm, whereas for PANI-HCl and PANI-TSA it was not possible to measure their average particle sizes by Coulter counter, mainly because their conductivities were comparable to that of the electrolyte used for dispersing the specimen powder. For PANI-DBSA, the average particle size was 20 μm, larger than that of the EB due to swelling by the large molecules of DBSA. Typical particle sizes of commercial polyaniline emeraldine salt (doped with sulfonic acid, Aldrich) are in the range 3–100 μm.

3.1.6. Conductivity measurements of PANI-salt powders

The electrical conductivities for the emeraldine salts PANI-HCl, PANI-TSA, PANI-DBSA (pressed pellet) were 12, 4 and 0.8 S cm^{-1} respectively. Conductivities of pressed pellet samples have previously been reported to be 3.3×10^{-1} S cm^{-1} for PANI-HCl and 1.1×10^{-4} S cm^{-1} for PANI-DBSA [14], which are much lower than our results.

Pure PANI-HCI showed the highest conductivity, probably due to the small size of Cl^- ions within the matrix. TSA and DBSA are bulky dopants that may interrupt the conductive pathways between the polymer chains. However, this deficiency is compensated to some extent by the improved self-organisation, thermal stability and processability caused by using the larger dopants. It is thought that DBSA dopant molecules are selectively bonded to the iminic nitrogens of PANI via proton transfer, whereas any "free" DBSA molecules are expected to be strongly hydrogen bonded to the aminic nitrogens and to other hydrogen bonding acceptors [20].

3.1.7. Solubility and miscibility

Simple qualitative solubility tests for PANI powders were carried out using the common organic solvents tetrahydrofuran (THF), dichloromethane (CH_2Cl_2) and chloroform ($CHCl_3$). Emeraldine base and PANI-DBSA were highly soluble in all of the above solvents giving dark blue and dark green solutions respectively. In contrast, PANI-HCl and PANI-TSA, showed little or no solubility, and solutions were either pale yellow for PANI-HCl or pale green for PANI-TSA. Similar results have been reported for EB and PANI-TSA [21], for PANI-HCl [19] and for PANI-DBSA [5].

In order to achieve a good miscibility between a PANI-salt and a solvent, their solubility parameters clearly have to be comparable. The solubility parameter $(J/cm^3)^{0.5}$ for THF is 20.3, and for chloroform is 19.0, whereas those calculated for EB and PANI-DBSA are 20.8 and 21.4 [17]. All these are comparable, and therefore it is expected that EB and PANI-DBSA would be soluble in THF and chloroform. The solubility parameter has been calculated for PANI-TSA to be 23.9 [22], which is somewhat further from those of THF and chloroform, and so it is expected to be insoluble in both of these solvents.

For PMMA, the solubility parameter is 19.0 [18], which is quite compatible with that of PANI-DBSA. Hence a considerable degree of mutual solubility is anticipated, and at low concentration we observe a homogeneous dispersion of the conducting polymer in PMMA. At the higher PANI-DBSA concentrations used for most of the blends, the bulk of the conductive polymer is present as discrete particles, but the interface between the polymers is probably very diffuse. Indeed, Zilberman *et al*. [17] have proposed that the surfaces of PANI-DBSA particles dispersed in polar polymer matrices are extended into nano-sized fibrils.

TABLE IV Conductivities (S cm^{-1}) of low flow and high flow areas in plaque sample of 15% PANI-TSA-7.5%HQ-PMMA

Sample	Low flow area	High flow area
Parallel to the flow	0.1227	0.0098
Perpendicular to the flow	0.0740	0.0159

3.2. PANI-plaques

3.2.1. Conductivity measurements

3.2.1.1. PANI-salt-PMMA plaques. On analysing the distribution of dc conductivity in the various samples, it was observed that regions of maximum flow during the moulding process invariably showed lower conductivities than those of low flow. Typical values are shown in Table IV. We propose that these observations may be explained by the flow-induced alignment of the surface fibrils and its consequent effect on the interparticle contact between PANI-DBSA particles. Fig. 2a and b illustrate the orientation of the surface fibrils in low- and high-flow regions respectively, for compositions in which the particles are not all in direct contact. In case (a) a conductive path is assured by good interfibrillar contact, and the bulk conductivity is virtually isotropic; whereas in case (b) the contact is attenuated even in the flow direction, and more so in the perpendicular direction. Note: It should be stressed that all conductivities quoted below are maximum values obtained in regions of low or zero flow.

A few preliminary blends of PANI-HCl and PANI-TSA at 20% loading without a plasticiser were processed by both compression and injection moulding and their respective conductivities (S cm^{-1}) were as follows: for 20% PANI-HCl, 0.032 and

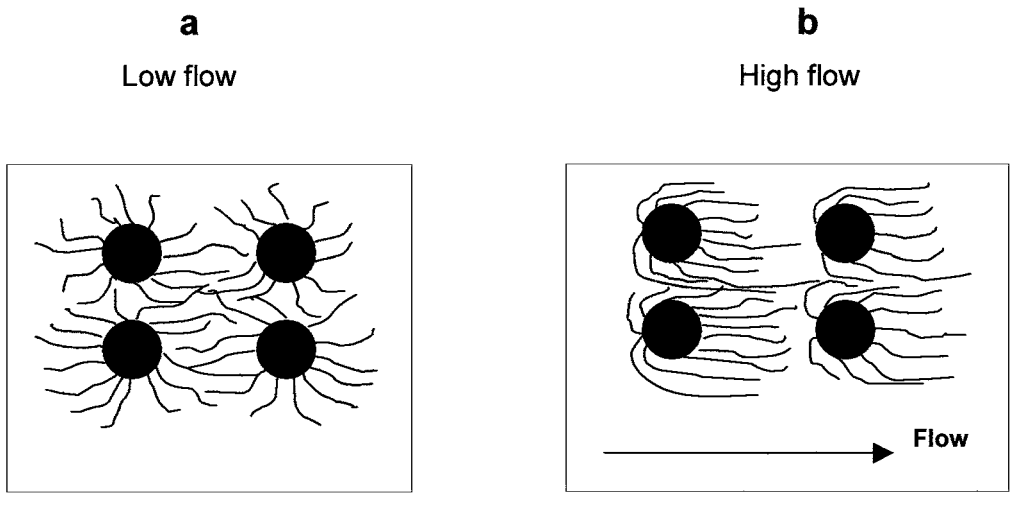

Figure 2 Representation of proposed effect of flow on interparticle contact in PANI-DBSA dispersion in an insulating host polymer.

3.1×10^{-13} S cm^{-1} and for 20% PANI-TSA, 0.015 and 1.9×10^{-13} S cm^{-1}. For pure PMMA (Sigma-Aldrich), the conductivity was found to be 1.7×10^{-13} S cm^{-1}. These results were lower than anticipated, especially for the injection-moulded samples. The following remarks can be made:

1. PANI-HCl composites were always more conductive than those of other PANI salts, as previously mentioned for the pure PANI samples.
2. During injection moulding, the blends might have been exposed to unnecessarily high temperatures that caused deprotonation and eventual destabilisation of the PANI-salt. At the same time, these samples would have undergone more shear-flow stress, which is likely to inhibit the formation of a good conducting pathway or network.

Although the percolation thresholds were not yet defined at this stage, they can be estimated to be between 10–15% for PANI-HCl and about 20% for PANI-TSA.

3.2.1.2. PANI-salt-PMMA-plasticiser plaques. In this work, several types of dihydroxybenzenes were investigated as plasticisers at various loadings to optimise the conductivities of the PANI-blends. Hydroquinone (HQ) was found to be the most effective, with the best conductivity at 7.5 wt% loading (see Fig. 3). Since our preliminary results were better for the compression-moulded plaques, most of the subsequent PANI samples were prepared by this process, although injection moulding would be preferred for industrial purposes. Several compositions of PANI-DBSA and PANI-TSA were blended with PMMA and the plasticiser HQ (7.5 wt%), and their electrical conductivities were compared (see Fig. 2). The percolation threshold appears to be 15% for PANI-TSA and 20% for PANI-DBSA. Plaques of PANI-DBSA-PMMA-HQ were less conductive than those of the PANI-TSA composites, and this can probably be explained as follows:

In general, the conductivities of the PANI blends are likely to be determined by the interaction between the PANI, the counter-ion and the other components present. There may be polar interactions with excess protonic acid, or with any neutral surfactant-type compounds with strong hydrogen bonding at one end and an organic tail compatible with solvent at the other end. Hydrogen-bonding donors include the phenolic hydroxyl groups OH, whereas the hydrogen-bonding acceptor is PANI itself (through the NH) or the sulphonic acid dopant (SO_3^-) [10].

The use of a plasticiser improves the conduction of the blends and lowers the percolation threshold. Good conductivities are thought to result from the "compatibility" of the PANI with the dopant and the plasticiser. This can lead to phenyl stacking mediated by hydrogen bonding and to charge transfer interaction between PANI-chains, counter-ion and the plasticiser, as proposed by other researchers [10, 22] for PANI doped with MSA, TSA, CSA or DBSA.

The conductivity of doped polymers normally decreases with increasing length of the side chains and the degree of substitution, but may actually increase with layer formation via phenyl stacking [13].

Another factor that could influence the conductivity, is the thermal treatment of the PANI blends. For example, the conductivity of PANI-DBSA has previously been found to increase roughly exponentially with annealing temperature from 1.1×10^{-4} S cm^{-1} at room temperature to 0.3×10^{-1} S cm^{-1} at 140°C, but it slowly decreased to 10^{-2} S cm^{-1} on cooling [14]. This was interpreted as being due to additional thermal doping and the formation of a well-defined layered structure. However, above 200°C thermal decomposition commences, causing a decrease in the conductivity.

3.2.2. Rheological measurements

From the rheological testing carried out on blends of PANI-DBSA-PMMA-HQ, it was found that pure PMMA had a higher viscosity than the PANI blends. The PANI-DBSA blends (15–40% loading) all showed a very similar dependence of viscosity on the shear rate. Hydroquinone as a plasticiser slightly decreased the viscosity of both pure PMMA and the PANI blends, and consequently, the processing of the blends was easier with the use of a plasticiser.

The viscosity of the blends decreased with increasing concentration of PANI-DBSA up to 25 wt%. Above this point, the viscosity increased significantly, and it seems likely that this can be ascribed to the appearance of extensive inter-linking of the surface fibrils on the PANI-DBSA particles, also associated with the onset of a rapid increase of electronic conductivity shown in Fig. 4.

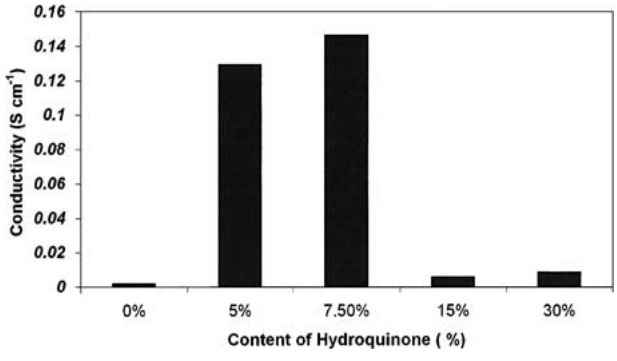

Figure 3 Conductivities of blends with different percentages of Hydroquinone.

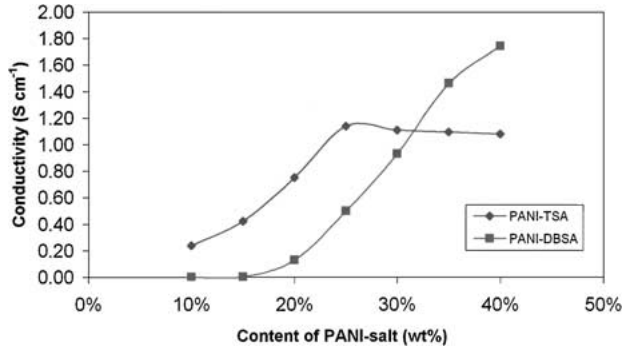

Figure 4 Comparison between conductivities of PANI-TSA and PANI-DBSA blends with PMMA and HQ at different loading.

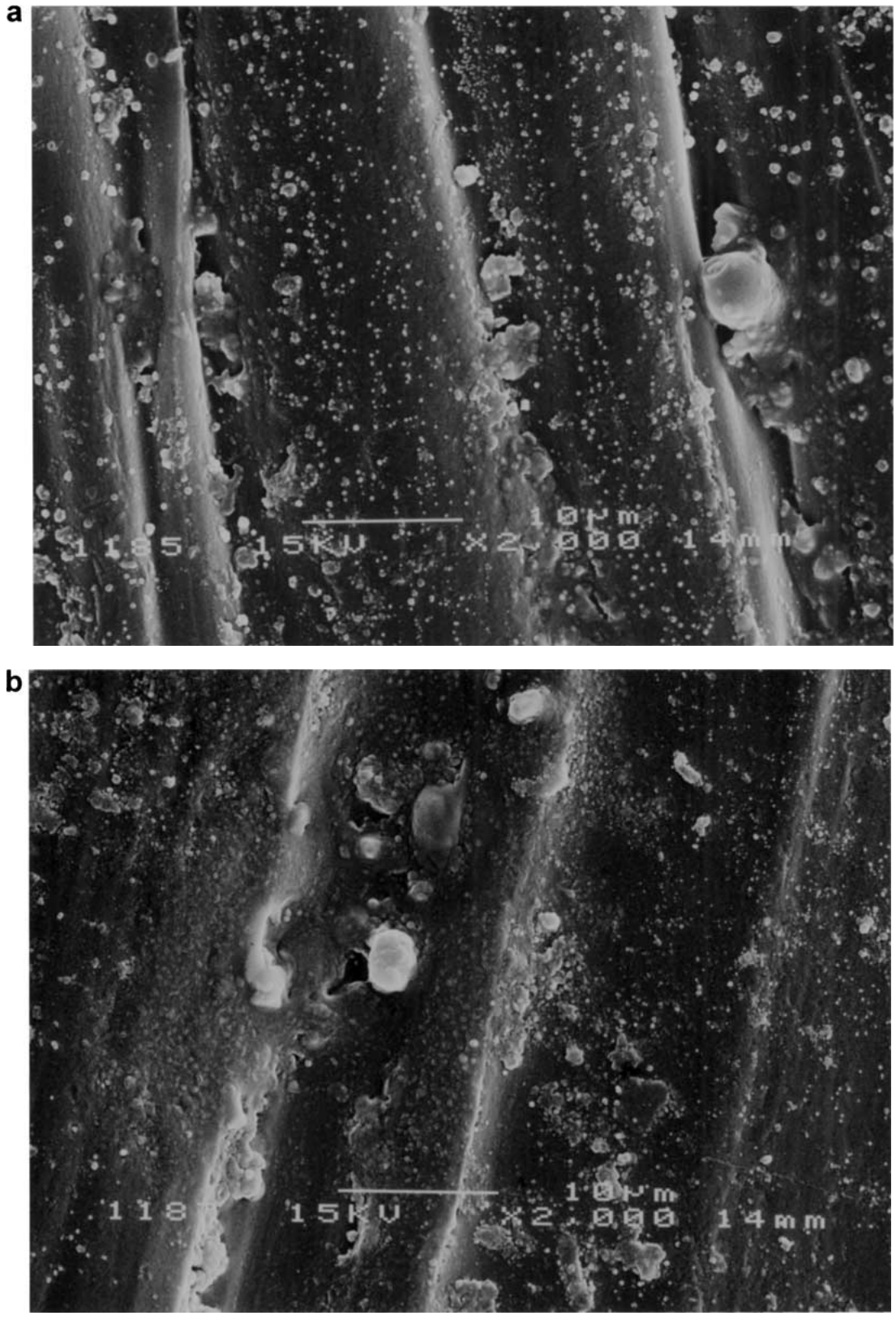

Figure 5 SEM micrographs of 20% PANI-blends with PMMA, (a) PANI-HCl and (b) PANI-TSA.

3.2.3. SEM

The transport properties of the conducting polymers are related to their microstructure and depending on the network of conducting pathways. Scanning electron microscopy was employed to study the possible effects of differences in morphology on the polymer blend conductivities. Various samples of 20% PANI-HCl-PMMA and 20% PANI-TSA-PMMA plaques were examined, but SEM micrographs at 2000× magnification showed no significant difference in their appearance. Both had surface striations and particles of PANI scattered along or between them, within a homogeneous background of the PMMA matrix (see Fig. 5). Elemental X-ray analysis by SEM-EDAX was carried out to identify the areas of PANI and PMMA. The specimens were coated with carbon for this purpose and particles along and between the striations within the matrix were analysed. Atomic percentages of CI were

higher in the particles than in the matrix areas, which suggests that the particles were PANI-HCl. Oxygen and nitrogen analyses were not very effective, since the N peak fell between those of C and O, and was difficult to quantify. The atomic percentages of N and Cl were 21.63 and 4.65% in the PANI-HCl plaque and those of N and S were 24.39 and 4.11% in PANI-TSA. These values are much lower than the results obtained by the full elemental analysis due to the fact that HCl and TSA are volatile under SEM beam heating.

3.2.4. Concluding remarks

The synthesis of emeraldine salt (PANI-HCl) under controlled pH and temperature was successfully scaled up by a factor of about 100 from the normally laboratory quantities. The degrees of protonation of EB as a result of using excess DBSA and TSA were determined to be 40–50%.

The highest conductivities were obtained for pure PANI-HCl, followed by PANI-TSA and PANI-DBSA. Although PANI-HCl is highly conductive, it is relatively thermally unstable compared to PANI-TSA and PANI-DBSA, since de-doping commences at 100°C, whereas for PANI-TSA and PANI-DBSA it is around 260°C. Furthermore, PANI-TSA and especially PANI-DBSA showed better compatibility with the host polymer, PMMA.

In general, compression moulded PANI blends showed much better conductivities than injection moulded ones. Highly conductive compression moulded blends were achieved with 15% loading of PANI-TSA and PANI-DBSA, but similar blends (even with 20% loading) gave very poor conductivities when processed by injection moulding.

The use of plasticisers improves the blending and processing of PANI with PMMA, (especially for hydroquinone), through hydrogen bonding and phenyl stacking, which allow better charge transfer between the PANI chains.

In summary, in order to achieve high conductivities, these factors have to be considered: the use of a plasticiser, restriction of the processing temperature to about 180–200°C (according to the duration of the processing), and intimate mixing of the constituents.

We are currently casting some PANI-DBSA blend films from solution to compare their conductivities with those of blends obtained by compression moulding. Further work also in progress on the possibility of processing conducting PANI blends by injection moulding.

Acknowledgement

The authors would like to thank both Kingston University and the University of North London for supporting this work. We would also like to thank Mike Fitzgibbon, Diambu Pappy-Mbikay and Koi Shing Ng of UNL for their contribution to the project, preparing blends and carrying out some rheological testing.

References

1. F. LUX, *Polymer* **35**(14) (1994) 2915.
2. D. C. TRIVEDI, in "Handbook of Organic Conductive Molecules and Polymers," Vol. 2, Conductive Polymers: Synthesis and Electrical Properties, edited by H. S. Nalwa (John Wiely & Sons, New York, 1997) p. 506.
3. A. G. MACDIARMID, *Synthetic Metals* **84** (1997) 27.
4. A. G. MACDIARMID, J. C. CHIANG, A. F. RICHTER, N. L. D. SOMASIRI and A. J. EPSTEIN, in Proceedings of the Workshop on the Conducting Polymers, Sintra, Portugal, July 1986, edited by L. Alcacer (D. Reidel publishing Co., 1987) p. 105.
5. D. ICHINOHE, T. ARAI and H. KISE, *Synthetic Metals* **84** (1997) 75.
6. L. M. GAN, C. H. CHEW, H. S. O. CHAN and L. MA, *Polymer Bulletin* **31** (1993) 347.
7. W. A. GAZOTTI JR, R. FAEZ and M-A. DE PAOLI, *European Polymer Journal* **35** (1999) 35.
8. J. STEJSKAL, M. SPIRKOVA, O. QUADRAT and P. KRATOCHVIL, *Polymer International* **44** (1997) 283.
9. L. W. SHACKLETTE, C. C. HAN and M. H. LULY, *Synthetic Metals* **57** (1993) 3532.
10. T. VIKKI, L-O. PIETILA, H. OSTERHOLM, L. AHJOPALO, A. TAKALA, A. TOIVO, K. LEVON, P. PASSINIEMI and O. IKKALA, *Macromolecules* **29** (1996) 2945.
11. P. N. ADAMS, P. J. LAUGHLIN and A. P. MONKMAN, *Synthetic Metals* **76** (1996) 157.
12. L. J. VAN DER PAUW, *Philips Research Reports* **13** (1958) 1.
13. W-Y. ZHENG, K. LEVON, T. TAKA, J. LAAKSO and J-E. OSTERHOLM, *Polymer Journal* **28**(5) (1996) 412.
14. S. KIM, J. M. KO and I. J. CHUNG, *Polymers for Advanced Technologies* **7** (1996) 559.
15. D. BLOOR and A. MONKMAN, *Synthetic Metals* **21** (1987) 175.
16. T. HJERTBERG, W. R. SALANECK, I. LUNSTROM, N. L. D. SOMASIRI and A. G. MACDIARMID, *J. Polym. Sci., Polym. Lett. Ed.* **23** (1985) 503.
17. M. ZILBERMAN, G. I. TITELMAN, A. SIEGMANN, Y. HABA, M. NAKRIS and D. ALPERSTEIN, *J. Appl. Polym. Sci.* **66** (1997) 243.
18. L. TERLEMEZYAN, M. MIHAILOV and B. IVANOVA, *Polymer Bulletin* **29** (1992) 283.
19. X. TANG, Y. SUN and Y. WEI, *Makromol. Chem., Rapid Commun.* **9** (1988) 829.
20. O. T. IKKALA, L.-O. PIETILA, P. PASSINIEMI, T. VIKKI, H. OSRTERHOLM, L. AHJOPALO and J.-E. OSTERHOLM, *Synthetic Metals* **84** (1997) 55.
21. Z. LI, Y. CAO and Z. XUE, *ibid.* **20** (1987) 141.
22. M. ZILBERMAN, A. SIEGMANN and M. NAKRIS, *J. Macromol. Sci.-Phys. B* **37**(3) (1998) 301.

Received 24 October 2000
and accepted 3 August 2001